

Variable Speed Wind Turbine Modeling for the Power Flow Analysis

Rudy Gianto*

Abstract—The use of variable speed wind turbines (*pembangkit listrik tenaga bayu*, PLTB) for electricity generation has increased. It contrasts with the fixed-speed PLTB, whose usage is decreasing. The major reason for PLTB's rapid development is that it has better wind power extraction or collection capabilities than the fixed-speed PLTB. Variable speed operation in a PLTB can be achieved using a doubly-fed induction generator (DFIG) application as the primary energy converter. The crucial initial step in investigating and analyzing power system containing PLTB that must be done is modeling all the components of the power system (including PLTB). An analysis of this power system is mostly conducted to evaluate its performance or appearance. This paper discusses the DFIG-based modeling of the variable speed PLTB to be applied in a power flow analysis of electric power systems. The proposed PLTB model was obtained based on formulas that calculate the power and power losses of the PLTB. The typically challenging power electronics converters modeling of DFIG was not required during the process of building the model. It differs from the previously reported methods in which two different models must be used to accommodate the power flow analysis in subsynchronous or super synchronous conditions. In this paper, the DFIG-based PLTB is represented through a mathematical model. This model could be used to express the DFIG, either in the subsynchronous or super synchronous conditions. It was subsequently integrated into the power flow analysis to evaluate the system's steady-state performance. The results of this case study will be further presented in this paper. In this study, the application of the proposed methods in the interconnected powers system containing PLTB was then examined. The results confirm the validity of the proposed DFIG model.

Keywords—Wind Turbine, DFIG, Power Flow Analysis, Power System.

I. INTRODUCTION

Variable speed wind turbines (*pembangkit listrik tenaga bayu*, PLTB) are now more frequently used to generate electricity. This increase occurs primarily due to the ability of the variable speed PLTB to extract or collect wind energy more optimally than the fixed speed PLTB.

A doubly-fed induction generator (DFIG) or permanent magnet synchronous generator (PMSG) can be used as the main energy converter to enable the variable speed operation in a PLTB. However, thanks to its lower cost, the DFIG application is more popular than that of PMSG [1]. To find out and analyze the energy system comprising PLTB, the system component

modeling of those energies (including PLTB) is required. Several techniques of PLTB modeling for the power flow analysis have been proposed. For instance, [2]-[16] have reported a number of the latest methods. References [2]-[4] have proposed the multi-node model of asynchronous generator-based PLTB for the power flow analysis. The proposed model could be applied to conventional power flow programs without modifying the programs' source codes. Yet, the programs' input data must be modified to incorporate PLTB in the power flow analysis. Additionally, methods in [2]-[4] could only be used for the fixed-speed PLTB.

Asynchronous generator-based PLTB for the power flow analysis has also been proposed [5], [6]. In both studies, the PLTB model was constructed according to the power balance of the asynchronous generator in the power system. A fixed-speed PLTB model based on the squirrel cage induction generator (SCIG) has been proposed in [7]. The model in [7] could be used for the power flow analysis of unbalanced distribution systems. References [8]-[12] have discussed various steady-state models of the fixed-speed PLTB for the power flow analysis. In the proposed method, the developed PLTB model was combined with the power flow formulation of the system without PLTB. This combined equation was then solved iteratively to obtain a solution to the overall power flow system problems. Same as in [2]-[4], methods proposed in [5]-[12] could not be applied to the variable speed PLTB.

Several research have proposed a DFIG-based PLTB model for the power flow analysis [13]-[16]. The steady-state model of the DFIG-based PLTB for the three-phase power flow analysis has been proposed [13], [14]. The model in [13] was developed based on the main components of the DFIG, namely wind turbines, power electronic converters, and induction generators. Meanwhile, the model in [14] was derived using the theories of sequence components. Another research has proposed an iterative approach to integrating the DFIG-based PLTB in the power flow analysis [15], [16]. Both research models were obtained from equivalent circuits of the DFIG, and the forward-backward sweeping (FBS) technique was employed to get solutions for power flow problems. However, in [13]-[16], two different models must be used to accommodate the power flow analysis in the subsynchronous and supersynchronous conditions.

This paper proposes the steady-state model of the variable speed PLTB, namely PLTB using the DFIG, for the power flow analysis. This model was obtained based on formulas to calculate the power and power losses of the PLTB. The typically-challenging power electronics converters modeling of DFIG was not required while building the model. In addition, using one mathematical model to represent the DFIG, either in subsynchronous or supersynchronous conditions, is another

*Jurusan Teknik Elektro, Fakultas Teknik, Universitas Tanjungpura, Jln. Prof. Dr. H. Hadari Nawawi, Pontianak 78124, INDONESIA (tel.: 0561-740186; email: rudygianto@gmail.com)

[Received: 24 April 2021, Revised: 11 March 2022]

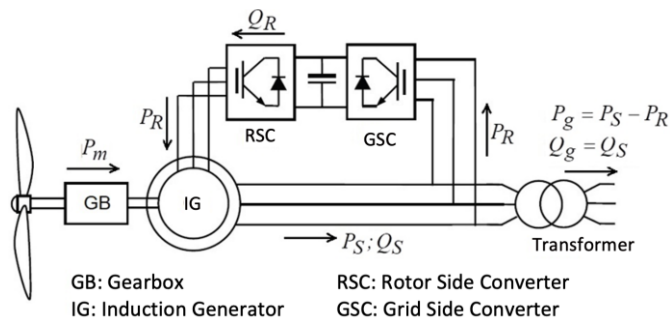


Fig. 1 DFIG-based PLTB configuration.

contribution of this paper. The proposed model was then integrated into the power flow analysis to evaluate the overall performance of the steady-state system (including PLTB).

II. DFIG-BASED PLTB

A. DFIG Structures and Equivalent Circuits of the DFIG

The DFIG system is currently the most popular type of PLTB. Its main component is the wound rotor induction generator (WRIG). Fig. 1 displays the base structure of the DFIG-based PLTB [17]-[22]. It can be observed that the stator winding of the WRIG is directly connected to the power system through an electronic converter via the slip rings. Since the power electronic converter controls the rotor circuits, the DFIG can import and export the reactive power.

In Fig. 1, P_m is the mechanical power of the turbine, P_S and Q_S are active and reactive powers on the stator of the WRIG, P_g and Q_g are active and reactive power outputs of the DFIG, P_R is the rotor power or power injected in the rotor, and Q_R is the reactive power generated by the WRIG. This reactive power is used to compensate for the reactive power necessitated by the WRIG for carrying out magnetization and supporting the reactive power requirements on the constant power factor operation.

It is important to note that the reactive power output of the DFIG (Q_g) will show negative or positive signs when it imports or exports the reactive power (DFIG operates on the lagging or leading power factor). When $Q_g = 0$, no reactive power is imported or exported by the DFIG (DFIG operates on the power factor of 1). Nevertheless, the DFIG is generally operated on the power factor of 1 [13]-[16] so that no reactive power exchange between PLTB and the power system (power grid). At the same time, the rotor power direction (P_R) depends on the WRIG rotor speed. In the supersynchronous condition, the rotor will send a power of P_R . However, in the subsynchronous condition, the rotor will absorb power equal to P_R . When the rotor speed is the same as the synchronous speed, namely $P_R = 0$, no power is sent or absorbed by the rotor.

The steady-state equivalent circuit of the WRIG is depicted in Fig. 2 [19], [20]. It should be noted that in Fig. 2, the reactive power is absent from the WRIG stator circuit, as it has been previously explained that the DFIG is usually operated at a power factor of 1 (or $Q_R = Q_S = 0$). In Fig. 2, V_S and I_S denote the voltage and current on the stator circuit, V_R and I_R are voltage and current on the rotor circuit, and s is slip in the induction generator. In addition, Z_S , Z_R , and Z_M are the

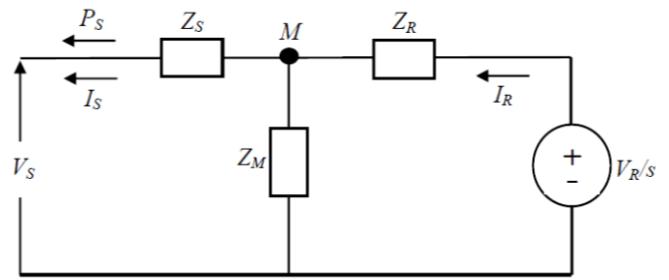


Fig. 2 Equivalent circuit of the DFIG steady state.

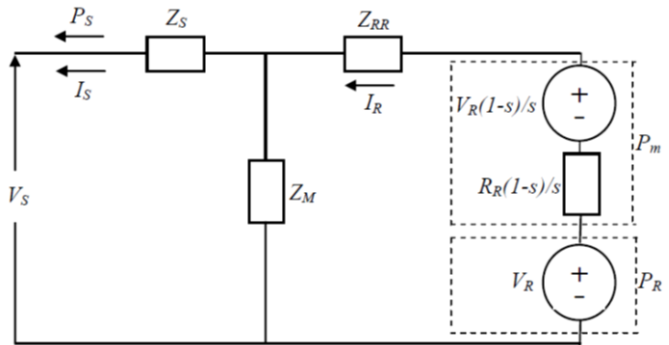


Fig. 3 Equivalent circuit of the modified DFIG steady state.

impedances of stator, rotor, and magnetic core circuits, which are calculated using (1).

$$\begin{aligned} Z_S &= R_S + jX_S \\ Z_R &= \frac{R_R}{s} + jX_R \\ Z_M &= jR_c X_m / (R_c + jX_m) \end{aligned} \quad (1)$$

where R_S and X_S are the resistance and reactance of the stator circuit, R_R and X_R are the resistance and reactance of the rotor circuit, while R_c and X_m are the resistance and reactance of the magnetic core circuit.

Fig. 3 also displays the steady-state equivalent circuit of the WRIG [19], [20]. In Fig. 3, modification to Fig. 2 is conducted to express the mechanical power of the turbine (P_m) and rotor (P_R) at the equivalent circuit of the WRIG [19], [20]. The Z_{RR} impedance in Fig. 3 is calculated using (2).

$$Z_{RR} = R_R + jX_R. \quad (2)$$

B. DFIG Power Formulation

Based on Fig. 1, the active and reactive power outputs of the PLTB is

$$P_g = P_S - P_R \quad (3)$$

and

$$Q_g = Q_S = 0. \quad (4)$$

After that, based on Fig. 2 and Fig. 3, the power on the WRIG stator circuit can be formulated using (5).

$$P_S = \text{Re}(V_S I_S^*) \quad (5)$$

meanwhile the active and reactive power on the WRIG rotor circuit is as follows [19], [20].

$$P_R = \text{Re}(V_R I_R^*) \quad (6)$$

and

$$Q_R = \text{Im}\left(\frac{V_R}{s} I_R^*\right) \quad (7)$$

where Q_R is the reactive power of the rotor as seen from the stator side.

Based on Fig. 3, the formulation for the mechanical power of the turbine is generated as follows [19], [20].

$$P_m = [\text{Re}(V_R I_R^*) - R_R I_R I_R^*] \frac{1-s}{s}. \quad (8)$$

Equation (8) shows that the turbine power of P_m has been expressed through the voltage source and dynamic resistance on the equivalent circuit in Fig. 3.

C. Formulation of the Current and Power losses of DFIG

It can be shown that the application of Kirchhoff's law to the current at M node of the equivalent circuit of the WRIG in Fig. 2 produces the stator current as in (9).

$$I_S = \left(1 + \frac{Z_R}{Z_M}\right) I_R - \frac{1}{sZ_M} V_R \quad (9)$$

and the rotor current:

$$I_R = \left(1 + \frac{Z_S}{Z_M}\right) I_S + \frac{1}{Z_M} V_S. \quad (10)$$

In addition, the application of Kirchhoff's law to the current on the loop of the equivalent circuit of the WRIG in Fig. 2 generates (11).

$$V_S - \frac{V_R}{s} + Z_S I_S + Z_R I_R = 0. \quad (11)$$

Based on (11), stator and rotor current can be expressed as follows:

$$I_S = \frac{1}{sZ_S} V_R - \frac{1}{Z_S} V_S - \frac{Z_R}{Z_S} I_R \quad (12)$$

and

$$I_R = \frac{1}{sZ_R} V_R - \frac{1}{Z_R} V_S - \frac{Z_S}{Z_R} I_S. \quad (13)$$

By substituting (13) on (9) and (12) on (10) as well as rearranging the results, stator and rotor currents can be declared as a function of the stator and rotor voltages as follows.

$$I_S = EV_R - FV_S \quad (14)$$

and

$$I_R = GV_R - HV_S \quad (15)$$

with

$$E = \frac{1}{s(Z_S + Z_R + Z_R Z_S / Z_M)} \quad (16a)$$

$$F = \frac{1 + Z_R / Z_M}{Z_S + Z_R + Z_R Z_S / Z_M} \quad (16b)$$

$$G = \frac{1 + Z_S / Z_M}{s(Z_S + Z_R + Z_R Z_S / Z_M)} \quad (16c)$$

$$H = \frac{1}{Z_S + Z_R + Z_R Z_S / Z_M}. \quad (16d)$$

Meanwhile the power losses on the WRIG, based on Fig. 3, is as follows

$$S_{loss} = I_S I_S^* Z_S + I_R I_R^* Z_{RR} + (I_R - I_S)(I_R - I_S)^* Z_M \quad (17)$$

or

$$S_{loss} = I_S I_S^* (Z_S + Z_M) + I_R I_R^* (Z_{RR} + Z_M) - (I_R I_S^* + I_S I_R^*) Z_M. \quad (18)$$

III. PLTB MODELING

This section discusses the formation of the proposed DFIG-based mathematical model of PLTB. The derivation of the model was based on the power and power loss of the DFIG. Since the active power losses of the WRIG is the difference between the mechanical power input of the turbine (P_m) and the electrical power output of PLTB (P_g), therefore

$$P_m - P_g = \text{Re}(S_{loss}) \quad (19)$$

meanwhile the reactive power generated by the rotor (Q_R) is to compensate the reactive power losses of the WRIG ($\text{Im}(S_{loss})$), hence

$$Q_R = \text{Im}(S_{loss}). \quad (20)$$

It is essential to note that in (19) and (20), the power losses on the power electronic converter are neglected since the value is smaller than that of power losses on the WRIG. The substitution of (3) on the (19) yields (21).

$$P_m - P_S + P_R = \text{Re}(S_{loss}). \quad (21)$$

Using (5) and (6) on (21) and (7) on (20) generates

$$P_m - \text{Re}(V_S I_S^*) + \text{Re}(V_R I_R^*) = \text{Re}(S_{loss}) \quad (22)$$

and

$$\text{Im}(V_R I_R^*) = s \text{Im}(S_{loss}). \quad (23)$$

Thus, based on (22) and (23), the proposed DFIG-based mathematical model of the variable speed PLTB is

$$P_m - \text{Re}(V_S I_S^*) + \text{Re}(V_R I_R^*) - \text{Re}(S_{loss}) = 0 \quad (24a)$$

$$\text{Im}(V_R I_R^*) - s \text{Im}(S_{loss}) = 0. \quad (24b)$$

It is noteworthy that in (24), S_{loss} was calculated through (18), while I_S and I_R was calculated according to (14) and (15). Since I_S and I_R is the function of the stator and rotor voltages, S_{loss} can also be regarded as the function of the stator and rotor voltage. In the formulation of power flow problems, this stator and rotor voltage was the quantity to be found or calculated. The mathematical model (24) was then integrated into the power flow analysis. The initial step in the integration process was to incorporate (24) into the following equation.

$$P_{Gi} - P_{Li} - \sum_{j=1}^n |V_i| |Y_{ij}| |V_j| \cos(\delta_i - \delta_j - \theta_{ij}) = 0 \quad (25a)$$

$$Q_{Gi} - Q_{Li} - \sum_{j=1}^n |V_i| |Y_{ij}| |V_j| \sin(\delta_i - \delta_j - \theta_{ij}) = 0 \quad (25b)$$

with

$$P_{Gi}, Q_{Gi} = \text{active and reactive power generation on the } i\text{th bus,}$$

TABLE I
BUS TYPE AND QUANTITY

Bus Type	Equation	Determined Quantity	Quantity Sought
Slack	(25)	$ Y , \theta, P_L, Q_L, V ,$ and $\delta = 0^\circ$	P_G and Q_G
PV	(25)	$ Y , \theta, P_L, Q_L, P_G,$ and $ V $	δ and Q_G
PQ	(25)	$ Y , \theta, P_L, Q_L,$ and $P_G = Q_G = 0$	$ V $ and δ
PLTB	(24) and (25)	$ Y , \theta, P_L, Q_L, \phi, s,$ and P_m	$ V = V_S , \delta = \delta_S, Re(V_R),$ and $Im(V_R)$

P_{Li}, Q_{Li} = need of the active and reactive power (load) on the i th bus,

$V_i = |V_i|e^{j\delta_i}$ = voltage on the i th bus,

$Y_{ij} = |Y_{ij}|e^{j\theta_{ij}}$ = i jth element of the bus admittance matrix,

N = the number of power system bus.

Equation (25) is the formulation of the power flow problem for the system without PLTB [23]. The following step was to complete the combined equations to obtain the solution to the intended power flow. Details of the equations to be completed and the electrical quantities to be calculated is shown in Table I. Since the stator voltage of the WRIG ($V_S = |V_S| \angle \delta_S$) was also the voltage at the PLTB terminal ($V = |V| \angle \delta$), for each PLTB bus, $|V| = |V_S|$ and $\delta = \delta_S$ was also quantities to be calculated. Furthermore, for each PLTB bus applied $P_G = P_g$ and $Q_G = Q_g = 0$. Power P_g can be calculated using (5) and (6) on (3) or

$$P_g = Re(V_S I_S^*) - Re(V_R I_R^*). \quad (26)$$

IV. CASE STUDY

A. Testing System

The study case was based on the 5-bus system adopted from the previous research [24]. This system had a three-phase total load of 810 MW and 400 MVAR. The system data are presented in Table II and Table III. This 5-bus system was then modified by integrating PLTB on bus 5 through a step-up transformer with an impedance of $j0.05$ pu (see Fig. 4). This PLTB comprised 100 units of identical generator turbines. The PLTB configuration can be seen in Fig. 4, while the unit data of generator turbines are shown in Table IV. In Table IV, the data in pu has a base of 200 MVA.

B. Calculation of Slip and Turbine Power

In this paper, it is assumed that the tip speed ratio (λ) value of the wind turbine is 8 and the coefficient of performance (C_p) is 0.5; therefore, based on (A.1) in the appendix, the mechanical power of the turbine for the various wind speed is

$$P_m = 0.5(1.225)(\pi 40^2)V_w^3(0.5) \quad (27)$$

meanwhile the generator slip (s) can be calculated using (L.4) in the appendix, namely

$$s = 1 - \frac{pV_w\lambda}{2\pi f s a_g R} \quad (28)$$

TABLE II
BRANCH DATA OF THE 5-BUS SYSTEM (IN PU)

Line	Bus p - q	Series Impedance (Z)	Shunt Admittance (Ysh/2)
1	1 - 3	0.042+j0.168	0
2	1 - 4	0.031+j0.126	0
3	2 - 3	0.031+j0.126	0
4	2 - 4	0.053+j0.210	0
5	2 - 5	0.084+j0.336	0
6	4 - 5	0.063+j0.252	0

TABLE III
BUS DATA OF THE 5-BUS SYSTEM (IN PU)

Bus	V	δ	Generation	Load*	Desc.
1	1.07	0	-	0.65+j0.30	Slack
2	1.06	-	1.8+j-	0.70+j0.40	PV
3	-	-	0	1.15+j0.60	PQ
4	-	-	0	0.85+j0.40	PQ
5	-	-	-	0.70+j0.30	PLTB

Desc.: - : quantity sought
* : load per phase

TABLE IV
UNIT DATA OF TURBINE-GENERATOR

Turbine	Power: 3,0 MW Length of turbine blade: 40 m Speed: Cut-in: 4 m/s; Rated: 13 m/s; Cut-out: 23 m/s
Gear	Ratio: 1/90
Generator	Type: DFIG Number of poles: 2 pairs Voltage: 690 Volt Resistance/Reactance (in pu*): $R_S = 1; X_S = 25; R_R = 1; X_R = 25; R_c = 3.000; X_m = 350$
Pad-mounted transformer	Impedance (in pu*): j5

or

$$s = 1 - \frac{(2)(8)V_w}{(100\pi)(1/90)(40)}. \quad (29)$$

Table V indicates the results of the calculation of the turbine mechanical power and slip for wind speeds, ranging from 5 m/s to 12 m/s.

C. PLTB Aggregation

To simplify the power flow analysis, groups of engine units (turbine-generator) in Fig. 4 were combined to form an equivalent single engine (the aggregation technique proposed in [4] was used for this purpose). In the PLTB with the representation of the single engine (see Fig. 5), the parameters of the equivalent WRIG are

$$\begin{aligned} R_{S,ek} &= 1/100 = 0.01 \text{ pu} \\ X_{S,ek} &= 25/100 = 0.25 \text{ pu} \\ R_{R,ek} &= 1/100 = 0.01 \text{ pu} \\ X_{R,ek} &= 25/100 = 0.25 \text{ pu} \\ R_{c,ek} &= 3000/100 = 30 \text{ pu} \\ X_{M,ek} &= 350/100 = 3.5 \text{ pu}. \end{aligned} \quad (30)$$

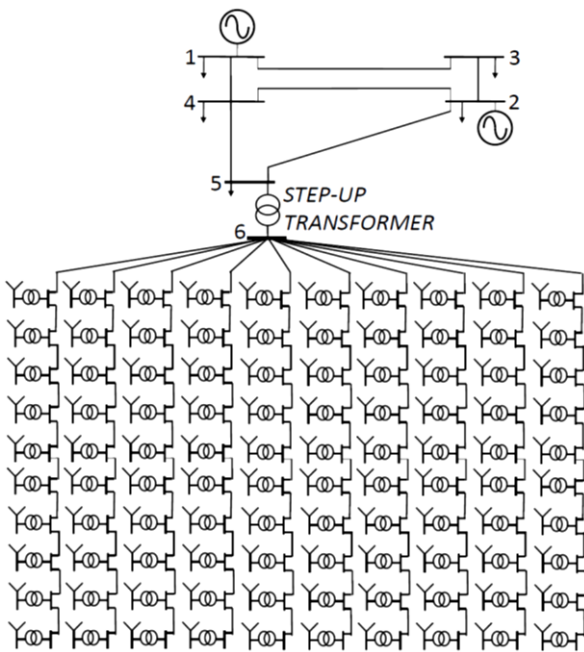


Fig. 4 Testing system.

TABLE V
GENERATOR SLIP AND MECHANICAL POWER OF THE TURBINE

V_w (m/s)	s	ΣP_m (MW)
5	0.4207	19.24
6	0.3125	33.25
7	0.1979	52.80
8	0.0833	78.82
9	-0.0313	112.22
10	-0.1459	153.94
11	-0.2605	204.89
12	-0.3751	266.00

At the same time, the impedance of the equivalent pad-mounted transformer is

$$Z_{T,ek} = j5/100 = j0.05 \text{ pu.} \quad (31)$$

D. Power Flow Calculation Results

The power flow study was conducted on the system in which PLTB was represented as an equivalent single engine (turbine-generator), as indicated in Fig. 5. The parameter values of the PLTB are as stated in (30) and (31). Results of the power flow analysis are shown in Table VI until Table VIII. To facilitate the observation, some of these results are presented in graphical forms, that are in Fig. 6 to Fig. 8.

The results of the power flow study found that the DFIG always delivered the reactive power (P_g) to the system (see column 2 in Table VI). This active power output was getting extensive as the mechanical power of the turbine (P_m) increased, but the value was slightly smaller when compared to the mechanical power of the turbine since there were power losses in the WRIG (see Fig. 6). This active power output was also the difference between the stator (P_s) and the rotor (P_R) active power of the WRIG. It is critical to note that in the subsynchronous operation, P_R was positive, or power equal to

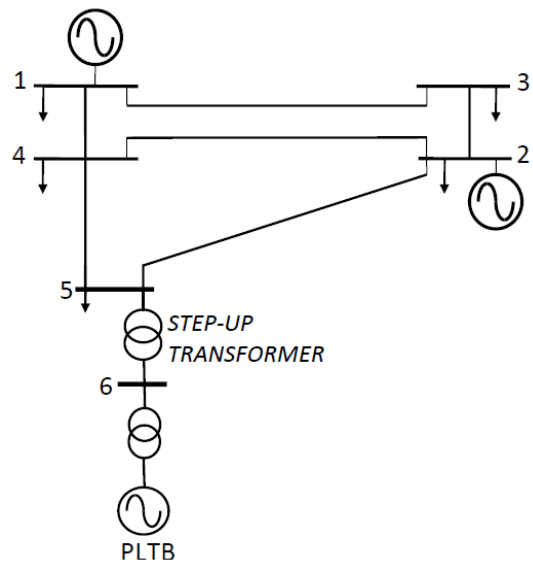


Fig. 5 Testing system (PLTB is represented as a single engine).

TABLE VI
FLOW DAN ACTIVE POWER LOSS OF THE DFIG

ΣP_m (MW)	P_g (MW)	P_s (MW)	P_R (MW)	P_{Loss} (MW)
19.24	12.91	27.46	14.55	6.33
33.25	26.71	42.12	15.41	6.54
52.80	45.95	59.39	13.44	6.85
78.82	71.53	79.28	7.76	7.29
112.22	104.33	101.78	-2.55	7.89
153.94	145.27	126.89	-18.38	8.67
204.89	195.23	154.59	-40.64	9.66
266.00	255.06	184.89	-70.17	10.94

TABLE VII
FLOW DAN REACTIVE POWER LOSS OF THE DFIG

ΣP_m (MW)	$Q_g = Q_s$ (MVAR)	Q_R (MVAR)	Q_{Loss} (MVAR)
19.24	0	58.50	58.50
33.25	0	62.41	62.41
52.80	0	68.62	68.62
78.82	0	77.80	77.80
112.22	0	90.67	90.67
153.94	0	108.17	108.17
204.89	0	131.56	131.56
266.00	0	163.12	163.12

PR was absorbed by the WRIG rotor. On the other hand, in the supersynchronous operation, P_R was negative, or power equal to P_R was delivered by the WRIG rotor (see column 4 in Table VI). The increase in the mechanical power of the turbine and the active power output of PLTB caused the increase in DFIG power losses due to the increase in current in the WRIG circuit (see Fig. 7).

Since DFIG operated at the power factor of 1, there was no reactive power exchange between the DFIG and the power system, or the value of $Q_g = 0$ (see column 2 in Table VII). Under these operation conditions, the reactive power produced by the WRIG rotor (Q_R) was entirely used to compensate for the reactive power required by the WRIG for magnetizing the

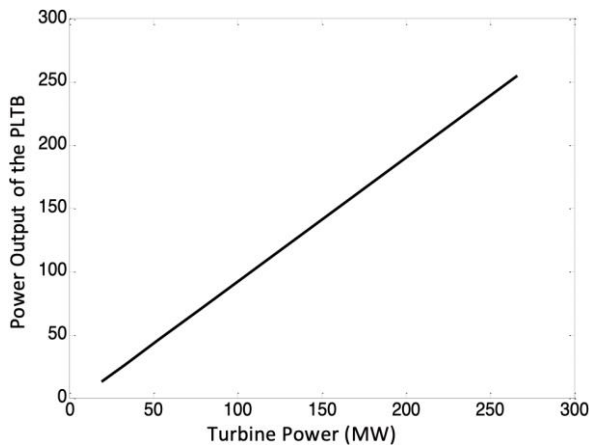


Fig. 6 Power output variations of PLTB.

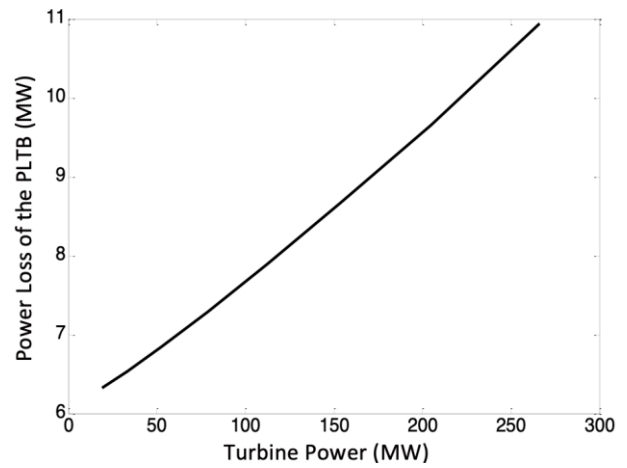


Fig. 7 Power loss variation of PLTB.

TABLE VIII
PLTB BUS VOLTAGE, OUTPUT OF G1+G2, LINE LOSSES

ΣP_m (pu)	Volt. (pu)	Output of G1+G2		Line Losses	
		MW	MVAR	MW	MVAR
19.24	0.9523	814.66	470.80	17.57	70.80
33.25	0.9566	799.51	465.69	16.22	65.69
52.80	0.9618	778.66	459.98	14.61	59.98
78.82	0.9674	751.40	454.78	12.92	54.78
112.22	0.9725	717.14	451.97	11.47	51.97
153.94	0.9756	675.46	454.32	10.73	54.32
204.89	0.9746	626.17	465.97	11.40	65.97
266.00	0.9654	569.47	493.37	14.53	93.37

induction generator core circuit (see column 3 in Table VII). The results of the power flow study also suggest that increasing the mechanical power of the turbine will also increase the active power output of the PLTB and the total active power generation of G1 and G2 will decrease (see Fig. 8). The decrease in active power generation of G1 and G2 occurs because some of the load can be supplied by the PLTB.

Results in Table VI to Table VIII confirm the validity of the proposed DFIG-based model of the PLTB. This validity can also be verified by observing the results; namely, the G1+G2 power plus the PLTB power ($P_g + jQ_g$) always equal the total system load plus line losses. It is noteworthy that lines in Table VIII were calculated based on the line impedances and currents flowing in the line.

V. CONCLUSION

The steady-state model of a variable speed PLTB (PLTB using DFIG) for the power flow analysis has been proposed in this paper. This model was obtained based on formulas calculating the power and power losses of the PLTB. The power electronic converter modeling of the DFIG, which is usually quite complex, was not required in the model building. Furthermore, the proposed model can be used to accommodate the power flow analysis, both in subsynchronous and supersynchronous conditions. This model was then integrated into the power flow analysis to evaluate the steady-state performance of the overall power system, including the PLTB. The results of the case studies have also been presented in this

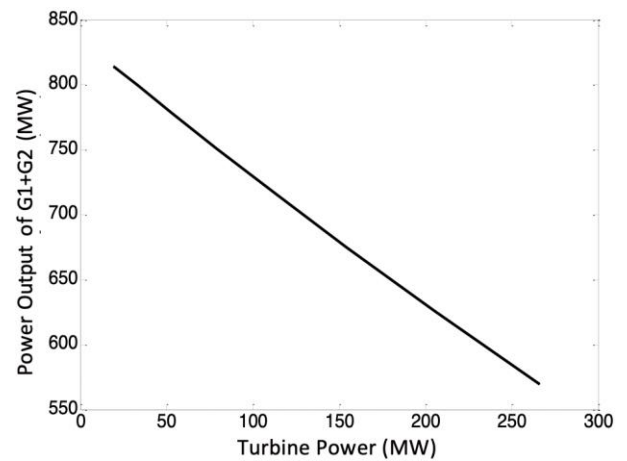


Fig. 8 Power output variation of G1+G2.

paper. In the case study, the application of the proposed method to an interconnected power system containing PLTB was investigated. The investigation results confirm the validity of the proposed DFIG model under subsynchronous and supersynchronous conditions.

CONFLICT OF INTEREST

Authors declare that there is no conflict interest in this paper.

APPENDIX

It is common knowledge that the wind turbine in the PLTB system functions to convert the kinetic energy of the wind into mechanical power. The amount of energy or mechanical power extracted or collected from this wind is given by (A.1) [17], [18].

$$P_m = 0.5\rho AV_w^3 C_p. \tag{A.1}$$

In (A.1), P_m is the mechanical power in watts, ρ is the air density in kg/m³ (for normal air conditions, the value is about 1.225 kg/m³), $A = \pi R^2$ (where R is the length of the turbine blades in meters), V_w is the wind speed (m/s), and C_p is the turbine performance coefficient.

The coefficient C_p is a function of the tip speed ratio (λ) and pitch angle (θ). This tip speed ratio has a typical value between

6-8 [17]. The turbine performance coefficient has the following general formula [18].

$$C_p = c_1 \left(\frac{c_2}{\lambda_i} - c_3 \theta - c_4 \theta^2 - c_5 \theta^3 - c_6 \right) e^{-c_7/\lambda_i} \quad (\text{A.2})$$

with

$$\lambda_i = \frac{1}{\frac{1}{\lambda + c_8 \theta} - \frac{c_9}{\theta^3 + 1}} \quad (\text{A.3})$$

and

$$\lambda = \frac{a_g \omega_R R}{p V_w} = \frac{a_g \omega_S (1-s) R}{p V_w}. \quad (\text{A.4})$$

In (A.4), a_g is the gear ratio, p is the number of pole pairs of the induction generator, ω_R is the angular velocity of the generator rotor (rad/s), $\omega_S = 2\pi f$ (where f is the system frequency), and s is the generator slip. It should also be noted here that the constants of c_1 to c_9 in (A.2) and (A.3) are determined based on data from wind turbine manufacturers, whereas the coefficient C_p in practice usually ranges from 0.4–0.5 [22].

REFERENCES

- [1] N.R. Babu and A. Arulmozhivarman, "Wind Energy Conversion System – A Technical Review," *J. Eng. Sci., Technol.*, Vol. 8, No. 4, pp. 493–507, Aug. 2013.
- [2] M.H. Haque, "Evaluation of Power Flow Solutions with Fixed Speed Wind Turbine Generating Systems," *Energy Convers., Manage.*, Vol. 79, pp. 511–518, Mar. 2014.
- [3] M.H. Haque, "Incorporation of Fixed Speed Wind Turbine Generators in Load Flow Analysis of Distribution Systems," *Int. J. Renew. Energy Technol.*, Vol. 6, No. 4, pp. 317–324, Jun. 2015.
- [4] J. Wang, C. Huang, and A.F. Zobaa, "Multiple-Node Models of Asynchronous Wind Turbines in Wind Farms for Load Flow Analysis," *Electr. Power Compon., Syst.*, Vol. 44, No. 2, pp. 135–141, Dec. 2015.
- [5] A. Feijoo and D. Villanueva, "A PQ Model for Asynchronous Machines Based on Rotor Voltage Calculation," *IEEE Trans. Energy Convers.*, Vol. 31, No. 2, pp. 813–814, Jun. 2016.
- [6] A. Feijoo and D. Villanueva, "Correction to 'A PQ Model for Asynchronous Machines Based on Rotor Voltage Calculation'," *IEEE Trans. Energy Convers.*, Vol. 31, No. 3, pp. 818–818, Jun. 2016.
- [7] A. Koksoy, O. Ozturk, M.E. Balci, and M.H. Hocaoglu, "A New Wind Turbine Generating System Model for Balanced and Unbalanced Distribution Systems Load Flow Analysis," *Appl. Sci.*, Vol. 8, No. 4, pp. 1–18, Mar. 2018.
- [8] R. Gianto, K.H. Khwee, H. Priyatman, and M. Rajagukguk, "Two-Port Network Model of Fixed-Speed Wind Turbine Generator for Distribution System Load Flow Analysis," *TELKOMNIKA*, Vol. 17, No. 3, pp. 1569–1575, Jun. 2019.
- [9] R. Gianto, "T-Circuit Model of Asynchronous Wind Turbine for Distribution System Load Flow Analysis," *Int. Energy J.*, Vol. 19, No. 2, pp. 77–88, Jun. 2019.
- [10] R. Gianto, "Model Ekuivalen-Pi dari Pembangkit Listrik Tenaga Angin dengan Generator Asinkron untuk Analisis Aliran Daya," *TRANSMISI*, Vol. 21, No. 4, pp. 103–108, Oct. 2019.
- [11] R. Gianto, "Integrasi Model Pembangkit Listrik Tenaga Angin pada Analisis Aliran Daya Sistem Tenaga," *J. Rekayasa Elektrika*, Vol. 16, No. 3, pp. 161–167, Dec. 2020.
- [12] R. Gianto, "Model Rangkaian-T Pembangkit Listrik Tenaga Bayu untuk Analisis Aliran Daya Tiga-Fase," *J. Nas. Tek. Elektro, Teknol. Inf.*, Vol. 10, No. 1, pp. 91–99, Feb. 2021.
- [13] A. Dadhanian, B. Venkatesh, A.B. Nassif, and V.K. Sood, "Modeling of Doubly Fed Induction Generators for Distribution System Power Flow Analysis," *Int. J. Elect. Power, Energy Syst.*, Vol. 53, pp. 576–583, Dec. 2013.
- [14] Y. Ju, *et al.*, "Three-Phase Steady-State Model of DFIG Considering Various Rotor Speeds," *IEEE Access*, Vol. 4, pp. 9479–9488, Dec. 2016.
- [15] V.S.S. Kumar and D. Thukaram, "Accurate Modelling of Doubly Fed Induction Based Wind Farms in Load Flow Analysis," *Electric Power Syst. Res.*, Vol. 15, pp. 363–371, Feb. 2018.
- [16] C.V.S. Anirudh and S.K.V. Seshadri, "Enhanced Modeling of Doubly Fed Induction Generator in Load Flow Analysis of Distribution Systems," *IET Renew. Power Gener.*, Vol. 15, No. 5, pp. 980–989, Apr. 2021.
- [17] O. Anaya-Lara, *et al.*, *Wind Energy Generation: Modelling and Control*. Chichester, England: John Wiley & Sons. Ltd., 2009.
- [18] T. Ackermann, Ed., *Wind Power in Power Systems*, Chichester, England: John Wiley & Sons. Ltd., 2012.
- [19] V. Akhmatov, *Induction Generators for Wind Power*. Brentwood, England: Multi-Science Publishing Co. Ltd., 2007.
- [20] I. Boldea, *Variable Speed Generators*. Boca Raton, USA: CRC Press, 2005.
- [21] B. Fox, *et al.*, *Wind Power Integration: Connection and System Operational Aspects*. London, England: The Institution of Engineering and Technology, 2007.
- [22] M.R. Patel, *Wind and Solar Power Systems*. Boca Raton, USA: CRC Press, 1999.
- [23] R. Gianto and K.H. Khwee, "A New Method for Load Flow Solution of Electric Power Distribution System," *Int. Rev. Electr. Eng.*, Vol. 11, No. 5, pp. 535–541, Oct. 2016.
- [24] W.D. Stevenson, *Elements of Power System Analysis*. New York, USA: Tata McGraw-Hill Book Co. Inc., 1992.